



The 65th ASH Annual Meeting Abstracts

POSTER ABSTRACTS

622.LYMPHOMAS: TRANSLATIONAL-NON-GENETIC

Investigating the Cell States and Prognostic Impact of Tumor Microenvironment Ecosystems in Classic Hodgkin Lymphoma

Shengqin Su¹, Ajay Subramanian², Timothy Flerlage, MD³, Jamie E. Flerlage, MDMS³, Stefan K. Alig, MD⁴, Everett J. Moding, MD PhD², Richard T. Hoppe, MD², Ranjana H. Advani, MD⁴, Yasodha Natkunam, MD PhD⁵, Ash A. Alizadeh, MDPH⁴, Michael S. Binkley, MD MS²

¹Department of Radiation Oncology, Stanford University School of Medicine, Palo Alto, CA

²Department of Radiation Oncology, Stanford University School of Medicine, Stanford, CA

³Department of Oncology, St. Jude Children's Research Hospital, Memphis, TN

⁴Department of Medicine, Divisions of Oncology and Hematology, Stanford University, Stanford, CA

⁵Department of Pathology, Stanford University School of Medicine, Stanford, CA

Introduction: Classic Hodgkin lymphoma (cHL) is distinguished from other cancers by the minute fraction of Hodgkin/Reed-Sternberg (HRS) cells (1-5%) in the tumor mass. Therefore, the immune-cell rich microenvironment plays a pivotal role in cHL's development, progression, and response to therapy. However, comprehensive characterization of the malignant and immune cell states in cHL has posed significant challenges due to the rarity of HRS cells and the intrinsic heterogeneity of the disease. To address this challenge, we aimed to characterize the immune cell states of cHL using a combination of experimental and bioinformatics approaches.

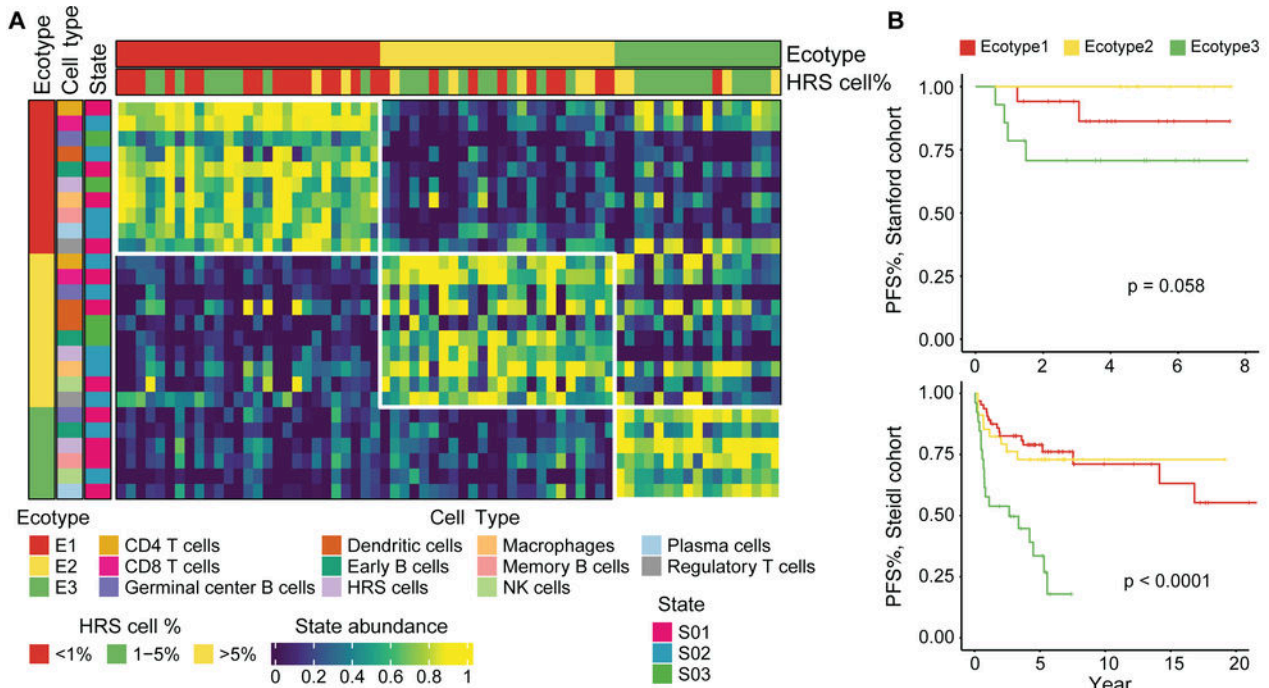
Methods: We identified patients diagnosed with cHL from 2013-19 managed at participating institutions with either formalin-fixed, paraffin-embedded (FFPE, $n = 89$) or cryopreserved cell suspensions prepared from excisional biopsies ($n = 5$). FACS purification of cell populations was performed on our cryopreserved tissues, followed by single cell RNA-seq (scRNA-seq) using 10X Genomics. Subsequently, we used CIBERSORTx to construct a customized signature matrix encompassing the gene expression profiles of 11 distinct cell types, including HRS cells. For our FFPE samples, we performed bulk RNA-seq with digital deconvolution using our signature matrix. Next, we combined the data and employed the EcoTyper machine learning framework to discover dominant cell states and ecosystems using deconvolved transcriptomics data. Validation of our identified cell states was performed in the remaining 2 samples with available scRNA-seq data, and a previously published cHL cohort ($n = 110$, Steidl et al. *NEJM* 2010).

Results: Using our discovery set of scRNA-seq samples ($n = 45,405$ cells), we identified distinct cell phenotypes including the HRS cells. Using these data, we developed a gene expression signature matrix allowing for the deconvolution of bulk transcriptomes from 89 cHL cases. Among 18 patients with tumor and cell-free somatic tumor mutation data, we observed a positive correlation between the HRS cell proportion and Variant Allele Frequencies (VAFs) from tumor or plasma DNA sequencing ($R = 0.71$ and 0.69 , respectively). Employing the EcoTyper framework, we discovered 26 unique cell states and three conserved cellular communities or "ecotypes" in the 68 bulk transcriptomes (Figure A). To validate the cell states identified in our EcoTyper model, we employed additional scRNA-seq on two validation samples ($n = 31,195$ cells) and spatial transcriptomics using Visium 10X ($n = 4$ tumors). We recovered the three established ecotypes and 26 cell states in these datasets and found a significant spatial autocorrelation of the ecotypes, verifying the biological validity of our EcoTyper model. Finally, we observed Ecotype-3 is associated with adverse progression-free survival in our cohort as well as an independent validation cohort (Figure B) after adjustment for clinical stage in a multivariable model ($HR = 8.78$, $P = 0.02$).

Conclusions: Our study represents a significant advancement in unraveling the complexities of the cHL cellular landscape. By leveraging innovative methodologies, we have shed light on key cell states and ecotypes within the tumor microenvironment that have prognostic significance, laying the groundwork for potential novel therapeutic avenues. Further validation in additional cohorts may allow ecotypes to risk stratify patients at diagnosis and aid in identification of poor performing subgroups within current low, intermediate, and high-risk groups.

Disclosures Flerlage: Seagen LLC: Research Funding. **Advani:** Incyte: Membership on an entity's Board of Directors or advisory committees; Epizyme: Membership on an entity's Board of Directors or advisory committees; Cyteir: Research Funding;

Gilead: Research Funding; Roche: Membership on an entity's Board of Directors or advisory committees; Merck: Research Funding; Genentech: Membership on an entity's Board of Directors or advisory committees; Beigene: Membership on an entity's Board of Directors or advisory committees; Regeneron: Research Funding; ADCT: Membership on an entity's Board of Directors or advisory committees, Research Funding; Seagen: Research Funding. **Alizadeh:** Janssen Oncology: Honoraria; CAPP Medical: Current holder of stock options in a privately-held company; Celgene: Consultancy, Research Funding; Foresight Diagnostics: Consultancy, Current holder of stock options in a privately-held company; Syncopation Life Sciences: Current holder of stock options in a privately-held company; Roche: Consultancy, Honoraria, Other: Travel, accommodations and expenses; Lymphoma Research Foundation: Consultancy; CiberMed: Consultancy, Current holder of stock options in a privately-held company; Forty Seven: Current holder of stock options in a privately-held company; Stanford University: Patents & Royalties: ctDNA detection; Gilead Sciences: Consultancy, Other: Travel, accommodations and expenses.



A) Heatmap visualization of 26 cell states and 3 ecotypes discovered in bulk transcriptomes. Top annotations denote ecotypes and percentage of Hodgkin/Reed-Sternberg (HRS) cells assigned to each patient. **B)** Survival plots comparing the progression free survival (PFS) among the three ecotypes. Survival data in top plot is collected from Stanford; survival data in bottom plot is obtained from Steidl et al. NEJM 2010.

Figure 1

<https://doi.org/10.1182/blood-2023-180288>